Available online at www.sciencedirect.com

SciVerse ScienceDirect

Ceramics International 39 (2013) 6827–6834

CERAMICS INTERNATIONAL

www.elsevier.com/locate/ceramint

Porous sodium borate-bonded SiC ceramics

Kwang-Young Lim[a], Young-Wook Kim[a,*], In-Hyuck Song[b]

[a]Functional Ceramics Laboratory, Department of Materials Science and Engineering, The University of Seoul, Seoul 130-743, Republic of Korea
[b]Engineering Ceramics Group, Korea Institute of Materials Science, Changwon 641-010, Republic of Korea

Received 28 December 2012; received in revised form 7 February 2013; accepted 8 February 2013
Available online 14 February 2013

Abstract

Porous silicon carbide ceramics were fabricated from SiC, sodium borate, and starch at temperatures as low as 650–800 °C by a simple pressing and heat-treatment process. The effects of heat treatment temperature and starch content on the porosity and strength of the ceramics were investigated. During heat treatment, the sodium borate transformed to a viscous phase, which acted as the bonding material between SiC particles, and the starch decomposed into gases, leaving pores. The porosity of the porous SiC ceramics could be controlled within a range of 47–64% with the present set of processing conditions. The porous SiC ceramics showed a maximum 64% porosity when 43.2 wt% SiC particles and 10.8 wt% sodium borate were used with 46 wt% starch. Flexural strength was at a maximum (37 MPa at 52% porosity) when the sintering temperature was 750 °C and the starch content was 40 wt%.

Keywords: B. Porosity; C. Strength; D. SiC; Sodium borate

1. Introduction

Porous silicon carbide (SiC) ceramics have been used and are considered one of the favorite materials for filters for molten metals, hot gases and diesel particulates, gas burner media, preforms for polymer- and metal-matrix composite fabrication, catalytic supports, refractory plates, and kiln furniture [1–18]. This is due to the properties these materials offer, such as low bulk density, excellent thermal shock and corrosion resistance, high specific strength, controllable permeability, and good creep resistance at high temperatures [19–23]. Porous SiC ceramics are most often produced by replica [4,7], direct foaming [24,25], sacrificial templates [13,26], reaction sintering [5,14], and partial sintering processes [10,11]. Different processing routes for porous SiC ceramics have been developed for specific applications to satisfy the associated porosity, pore size, and degree of pore interconnectivity requirements. However, all the above methods require high temperatures of ≥ 1400 °C for the processing if SiC powder is used as a starting material. Cost-effective production of porous SiC ceramics for low temperature (≤ 300 °C) applications such as grinding and light armor applications can be achieved by using coarse SiC powders as a starting material and processing the ceramics at lower temperatures.

Recently, the production of porous SiC ceramics from preceramic polymers has attracted considerable attention because of the expected improvement in porous ceramic properties and the potentially more cost-effective polymer processing [12,27]. The most important advantage of this method is the ease of preparation and low processing temperatures. A few researchers have fabricated porous SiC ceramics successfully at temperatures as low as 1000–1400 °C by a simple pressing and subsequent pyrolysis process using polycarbosilane as a precursor for SiC [28].

Another way to lower the processing temperature of SiC ceramics is the use of bonding materials. Silica (SiO_2), silicon nitride (Si_3N_4), mullite ($3Al_2O_3 \cdot 2SiO_2$), cordierite ($2MgO \cdot 2Al_2O_3 \cdot 5SiO_2$), silicon oxycarbide, and geopolymer phases were investigated as bonding phases for SiC ceramics. A silica bonding phase is formed by heating SiC powder compacts at 1100–1400 °C in air [29,30]. The SiC particles in the compacts are bonded to each other by oxidation-derived SiO_2 glass. A silicon nitride bonding phase is similarly formed by nitridation of the silicon (Si)

*Corresponding author. Tel.: +82 2 2210 2760; fax: +82 2 2215 5863.
E-mail address: ywkim@uos.ac.kr (Y.-W. Kim).

0272-8842/$ - see front matter © 2013 Elsevier Ltd and Techna Group S.r.l. All rights reserved.
http://dx.doi.org/10.1016/j.ceramint.2013.02.014

powder in compacts containing SiC and Si powders [31]. The processing temperature for the nitridation ranges from 1250 °C to 1450 °C. A mullite bonding phase is formed by the reaction between Al_2O_3 and oxidation-derived SiO_2 in compacts containing SiC and Al_2O_3 powders with heating at 1400–1550 °C in air [9,32]. During heating, the oxidation of SiC produces a SiO_2 phase, which reacts with Al_2O_3 to form a mullite bonding phase. A cordierite bonding phase is formed by the reaction between Al_2O_3, MgO, and oxidation-derived SiO_2 in compacts containing SiC, Al_2O_3, MgO, and graphite powders during heating at 1200–1400 °C in air [33]. A silicon oxycarbide bonding phase is formed by the pyrolysis of polysiloxane in compacts containing SiC, polysiloxane, and sacrificial templates [34–36]. However, the heat treatment temperatures required in the above studies were all ≥ 800 °C and the mechanical properties of the resulting ceramics were strongly dependent on the composition of the bonding materials [29–36]. Recently, porous alkali-bonded SiC ceramics were developed using a geopolymer as a bonding phase [37]. The bonding phase is formed from metakaolin in the presence of alkali solution. Metakaolin in alkaline conditions dissolved and reprecipitated to form geopolymeric nano-particles that act as a bonding phase to bind SiC particles together. However, the compressive strengths of the porous alkali-bonded SiC ceramics were very poor (< 1 MPa) [37].

Studies using sodium borate ($Na_2B_4O_7 \cdot 10H_2O$) as a bonding phase for SiC have not yet been reported. Sodium borate melts at a temperature below 750 °C and its density is 1.74 g/cm^3. Thus, it has several advantages as a bonding phase for SiC including (1) very low processing temperatures (650–800 °C); (2) light weight because of the low density of the bonding phase; and (3) the ability to use coarse (10 μm) SiC particles. The first and third advantages will lead to the greatest cost-effectiveness in the production of porous SiC ceramics.

This paper first reports the extremely low-temperature (650–800 °C) processing of porous, high-strength SiC ceramics using sodium borate as a binding material. In addition, the effects of the heat-treatment temperature and starch template content on the porosity and flexural strength of the fabricated porous ceramics are described.

2. Experimental

Commercially available refractory-grade α-SiC powders (~10 μm, Zhengxing Abrasive Co., Dalian, China), sodium borate ($Na_2B_4O_7 \cdot 10H_2O$, >99% pure, Samchun Pure Chemical Co., Ltd., Pyeongtaeck, Korea), and starch (Corn, Extra Pure, Samchun Pure Chemical Co., Ltd., Pyeongtaeck, Korea) were used as the starting materials. The starch was added as a sacrificial template. The effect of the starch content was examined by preparing three batches containing 40–46 wt% starch by ball milling. To investigate the effect of the template content, three batches were mixed, each containing SiC and sodium borate in an 8:2 weight ratio (see Table 1). All the batches were ball-milled separately in a polypropylene jar for 16 h using distilled water and SiC balls. Distilled water was used as a solvent for dissolving sodium borate. The dissolution of sodium borate was beneficial for making the powder mixture homogeneous. The milled slurry was dried, sieved, and pressed uniaxially under a pressure of 28 MPa. The pressed compacts were heat treated at 650–800 °C for 30 min in air at a heating rate of 2 °C/min. Thermal gravimetric analysis (TGA) and differential thermal analysis (DTA) for the decomposition of sodium borate was carried out up to 800 °C with a heating rate of 2 °C/min in air. The temperature measurement during the TGA/DTA experiments was made within ±0.5 °C.

Table 1
Batch composition and sample designation of porous SiC ceramics.

Specimen designation	Batch composition (wt%)		
	SiC[a] (~10 μm)	Sodium borate[b]	Starch[c]
SC40	48.0	12.0	40.0
SC43	45.6	11.4	43.0
SC46	43.2	10.8	46.0

[a] ~10 μm, Zhengxing Abrasive Co., Ltd., Dunhua, China.
[b] >99%, Extra pure, Samchun Pure Chemical Co., Ltd., Pyeongtaeck, Korea.
[c] Corn, Extra pure, Samchun Pure Chemical Co., Ltd., Pyeongtaeck, Korea.

The bulk density of the resulting ceramics was calculated from the weight-to-volume ratio of the samples. To measure flexural strength, bar-shaped samples were cut to a size of $4 \times 5 \times 35$ mm^3. Bend tests were carried out at room temperature on 7–10 specimens under each condition using a four point method with inner and outer spans of 10 mm and 20 mm, respectively, and a crosshead speed of 0.5 mm/min. The fracture surfaces were observed by scanning electron microscopy (SEM, S4300, Hitachi Ltd., Hitachi, Japan).

3. Results and discussion

Fig. 1 shows typical DTA and TGA curves in air for the thermal decomposition of sodium borate ($Na_2B_4O_7 \cdot 10H_2O$) supplied by Samchun Pure Chemical Co. The DTA curve shows three endothermic peaks and one exothermic peak. Fig. 2 shows XRD patterns of the as-received SiC powder, 800 °C-treated SiC powder, as-received sodium borate, and sodium borate heat-treated at 117, 200, 500, and 700 °C. From Figs. 1 and 2, several observations can be made.

From the DTA curve, the first endothermic peak at 81 °C was due to the partial loss of crystallization water from the hydrolyzed sodium borate (i.e., $Na_2B_4O_7 \cdot 10H_2O$ transformed to $Na_2B_4O_7 \cdot 5H_2O$ at 81 °C). XRD patterns (Fig. 2) of the as-received sodium borate and the 117 °C-treated sodium borate clearly show the loss of water from sodium borate. The second endothermic peak at 133 °C

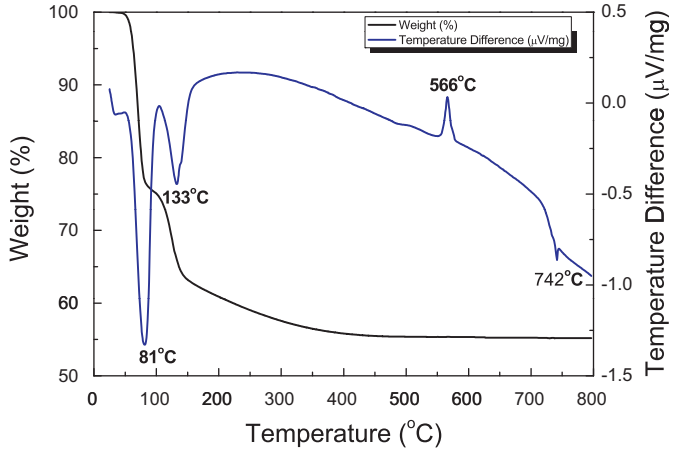

Fig. 1. Thermal gravimetric analysis (TGA) and differential thermal analysis (DTA) for sodium borate ($Na_2B_4O_7 \cdot 10H_2O$) heated to 800 °C in air.

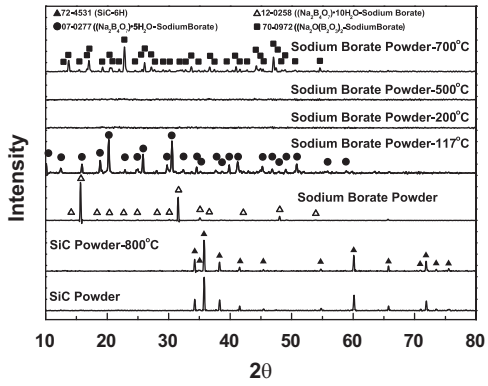

Fig. 2. X-ray diffraction spectra of the as-received and heat-treated sodium borates at various temperatures, a SiC starting powder, and a SiC powder heat-treated at 800 °C.

was due to the loss of the remaining crystallization water, leading to the formation of amorphous sodium borate. XRD patterns of the sodium borates treated at 200 °C and 500 °C show the presence of an amorphous phase without any evidence of crystalline phases (Fig. 2). The first exothermic peak at 566 °C was due to the crystallization of anhydrous sodium borate ($Na_2O(B_2O_3)_2$) from the amorphous phase. XRD data of the sodium borate samples heat treated at 500 °C and 700 °C clearly show this crystallization of the anhydrous sodium borate phase. The third endothermic peak observed at 742 °C was due to the melting of the crystalline anhydrous sodium borate phase.

From the TGA curve, the total weight loss between room temperature and 800 °C was ~46%, smaller than that of the theoretical value (~47%) derived from the chemical formula. This may be due to the presence of impurities in the sodium borate (the purity of the as-received sodium borate was ~99%) and the possibility of the presence of some $Na_2B_4O_7 \cdot 5H_2O$ in the as-received sodium borate.

Heat treatment of SiC powders at 800 °C showed no change in XRD peaks, as shown in Fig. 2. This was likely due to the fairly large particle size of the SiC powders (~10 μm), which showed negligible oxidation up to 800 °C in air.

The effect of sintering temperature on the microstructure of the porous SiC ceramics is shown in Fig. 3 for specimens containing 40 wt% starch template. The microstructures consisted of large SiC grains, the sodium borate bonding phase, and starch-templated pores. The pressed compacts were heat treated at 650–800 °C for 30 min in air at a heating rate of 2 °C/min. The heat treatment facilitated the starch decomposition that left pores and melting of the sodium borate "glue" to bind SiC particles together. As shown in Fig. 3(c) and (d), large SiC particles were well-bonded to each other by the molten sodium borate phase when the sintering temperature was higher than the melting temperature of sodium borate. Pore morphology in the samples sintered at 650 and 700 °C was irregular and the pores were formed between SiC particles, whereas most of the pores in the samples sintered at 750 and 800 °C were partially filled with porous amorphous sodium borate phase. The morphology of the pores embedded in the bonding phase (sodium borate) was spherical with a diameter of 1–3 μm. The small, spherical pores were formed by water vapor liberated from the sodium borate. The crystallization water in the sodium borate ($Na_2B_4O_7 \cdot 10H_2O$) thus acts as a blowing agent in the bonding phase.

Fractures in the samples heat-treated at 750 and 800 °C occurred mostly inside the bonding phase, i.e. sodium borate, resulting in a smoother fracture surface than the other samples. In contrast, fractures in the samples heat-treated at 650 and 700 °C were found mostly between SiC grains and the sodium borate bonding phase, resulting in more jagged fracture surfaces. This result suggests that the melting of sodium borate led to stronger bonding between SiC particles. Observed variation in bonding characteristics is believed to influence the strength of the porous ceramics.

Fig. 4 shows XRD spectra of the porous SiC ceramics sintered at various temperatures. As shown, samples sintered at 650, 700 and 750 °C showed no secondary phase formation after sintering. Crystalline anhydrous sodium borate phase ($Na_2O(B_2O_3)_2$) was not observed in the samples sintered at 700 °C. This might indicate that the presence of SiC could retard or suppress the crystallization of the $Na_2O(B_2O_3)_2$ phase from the amorphous sodium borate (see Fig. 2). However, the sample sintered at 800 °C showed the presence of a crystalline cristobalite phase (JCPDS 76-0941) in addition to 6H–SiC phase. This is inconsistent with the XRD pattern of the SiC powders heat-treated at 800 °C, shown in Fig. 2. Comparison of the XRD patterns of the sample sintered at 800 °C (Fig. 4) with that of the SiC powders heat-treated at 800 °C (Fig. 2) suggests that (1) the presence of molten sodium borate accelerates the oxidation of SiC particles, and (2) the oxidation of SiC particles results in the formation of sodium borosilicate glass during sintering at 800 °C in

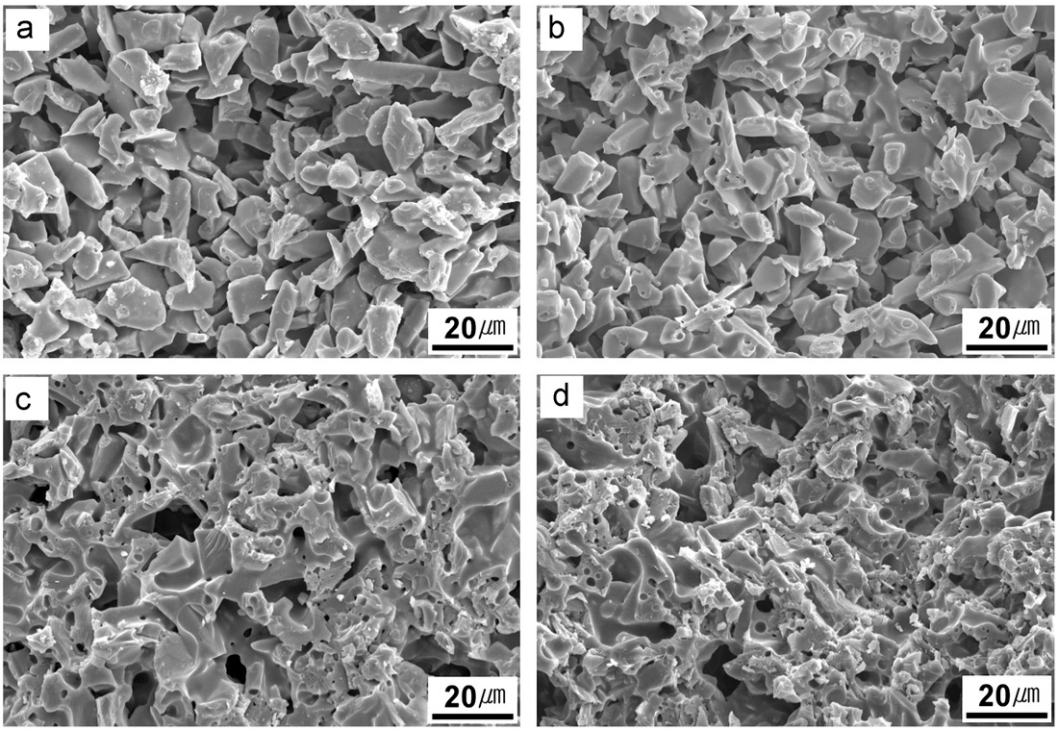

Fig. 3. Effect of sintering temperature on the microstructure of porous SiC ceramics. Each specimen contained 40 wt% starch as a template in the starting composition and was then sintered at the following temperatures: (a) 650, (b) 700, (c) 750, and (d) 800 °C.

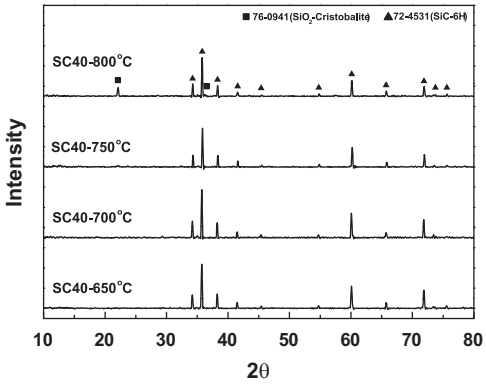

Fig. 4. X-ray diffraction spectra of porous SiC ceramics sintered at 650–800 °C for 30 min in air.

air, and (3) the cristobalite phase was precipitated from the glass during cooling from the sintering temperature. It is expected that molten sodium borate reacts with the surface silicon oxide film (SiO_2) of the SiC particles and enhance the exposure of naked SiC with oxygen, resulting in enhanced oxidation. It is noted that sodium borate remained amorphous in all samples sintered between 650 and 800 °C in air (see Fig. 4). Enhanced oxygen diffusion through the amorphous phase would then contribute to the accelerated oxidation of SiC particles in the specimen.

One alternative method for low-temperature processing of porous SiC ceramics is SiOC-bonded SiC ceramics [34–36]. Previous work on SiOC-bonded SiC ceramics produced severe cracking in the SiOC bonding phase when large SiC particles (10 or 15 μm) were used [36]. The greater volume reduction of the polysiloxane due to pyrolysis combined with the constrained SiC network resulted in residual tension within the structure, which resulted in cracking in the specimens. However, sodium borate transforms to a viscous solid or liquid phase—depending on the sintering temperature—with little volume shrinkage and binds together SiC particles; thus, no cracking was observed in the samples, even after furnace cooling, as can be seen in Fig. 3.

Fig. 5 shows typical microstructures of porous SiC samples heat-treated at 750 °C containing different proportions of starch. The porosity increased with increased starch content, as expected (this will be discussed further later). From the micrographs of Fig. 5, pore size also substantially increased with increased starch content. In addition, the number of large pores with a size range of 15–25 μm, which originated from the agglomerated starch, increased with increased starch content. More starch content led to more agglomeration in the batches and resulted in the increased pore size and the formation of more large pores in the microstructure.

Fig. 6 shows the porosity of the porous SiC ceramics as functions of the starch content and sintering temperature. Porosity increased from 47–57% to 50–64% as starch content increased from 40 wt% to 46 wt%. The increase in porosity was caused by the addition of more templates. At a constant starch content, the porosity generally decreased with increasing sintering temperature because

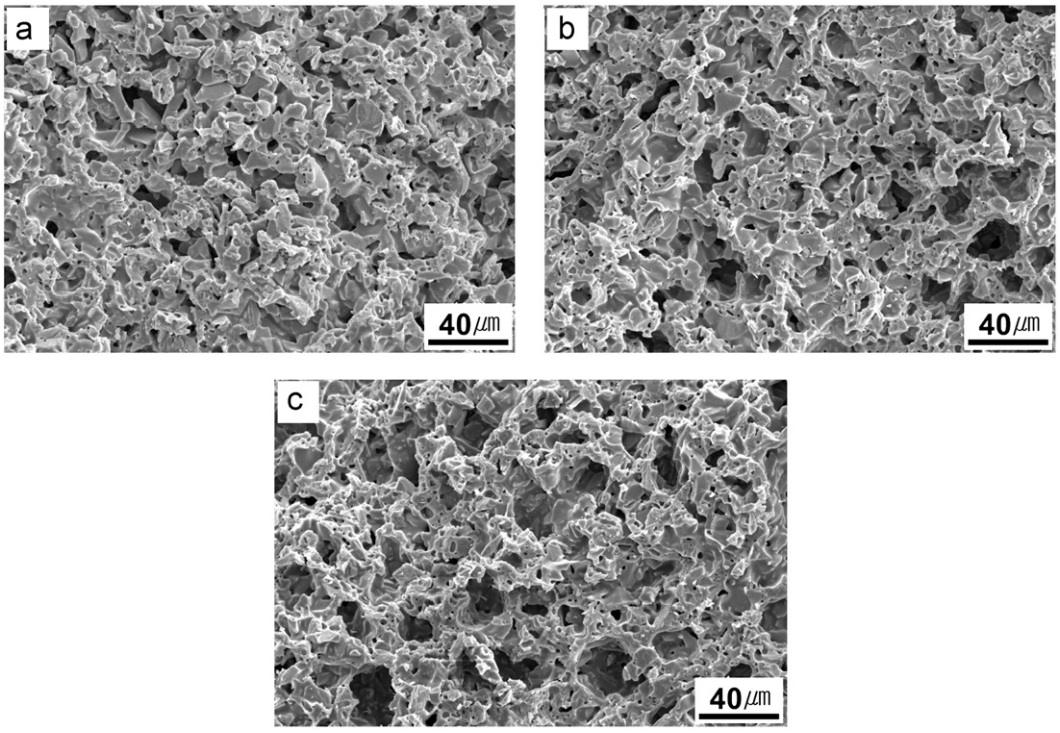

Fig. 5. Effect of starch content on the microstructure of porous SiC ceramics sintered at 750 °C for 30 min in air. Starch content of samples: (a) 40, (b) 43, and (c) 46 wt%.

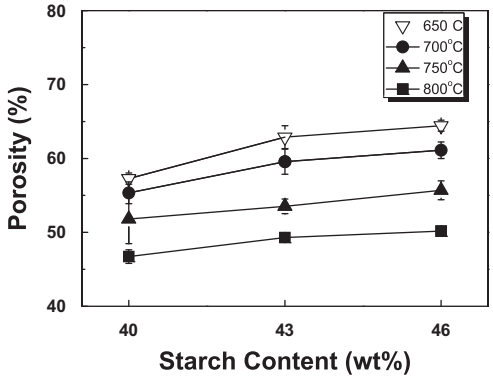

Fig. 6. Porosity of the porous SiC ceramics sintered at 650–800 °C for 0.5 h in air as a function of starch content.

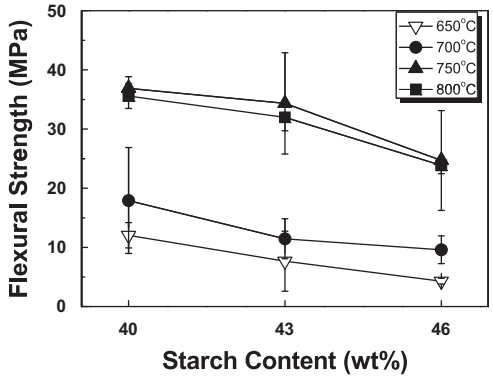

Fig. 7. Flexural strength of the porous SiC ceramics as a function of starch content.

of the partial filling of pores by viscous sodium borate flow. A maximum porosity of 64% was obtained when 46% starch was added and sintered at 650 °C. In contrast, a minimal porosity of 47% was obtained when 40% starch was added and sintered at 800 °C. The present results suggest that the porosity of porous sodium borate-bonded SiC ceramics can be controlled in a range of 47–64% by adjusting the starch content and the sintering temperature.

Fig. 7 shows the variation in flexural strength as a function of starch content and sintering temperature. The strength generally decreased with increasing starch content because of the increased porosity. The strength increased with increasing sintering temperature and showed maxima at 750 °C, and then decreased slightly at 800 °C for all samples, regardless of starch content. A maximum strength of 37 MPa was obtained when 40% starch was added and sintered at 750 °C. At the same starch content, samples sintered at 750 and 800 °C showed strength values 2–3 times greater than those of the samples sintered at 650 and 700 °C. This was due to the melting of the sodium borate bonding phase, which takes place at 742 °C (see Fig. 1). Thus, the state of the bonding phase was solid at 650 and 700 °C, whereas it was liquid at 750 and 800 °C. This difference made a difference in the bonding characteristics, which led to the large difference in the strength values. It was supported by the difference in fracture mode, as observed in Fig. 3.

It is well-documented that the flexural strength of porous ceramics decreases with increasing the porosity [12,30,38]. However, the opposite trend was observed in this research, in samples sintered at 750 and 800 °C. Although the 750 °C samples showed higher porosity (52–56%) than the 800 °C samples (47–50%) (Fig. 6), samples sintered at 750 °C showed higher strength (25–37 MPa) than those sintered at 800 °C (24–36 MPa) (Fig. 7). For example, the strength and porosity of the 750 °C sample containing 43% starch were 34 MPa and 54%, respectively. In contrast, those of the 800 °C-sintered sample containing the same amount of starch was 32 MPa and 49%, respectively. The decrease in the flexural strength of the samples sintered at 800 °C, compared to those sintered at 750 °C, could be due to the formation of oxidation product (SiO_2, cristobalite) in the samples, as identified by XRD (Fig. 4). The formation of cristobalite phase in the samples may deteriorate the bonding material (amorphous sodium borate) mechanically by removing SiO_2 at least partially from the amorphous sodium borosilicate glass and result in a decreased strength. In addition, the formation of cristobalite leads to the phase transformation and volume change during cooling, resulting in decreased strength. However, the degree of the strength degradation depends on the crystal size and content of cristobalite formed.

Fig. 8 presents the flexural strength data as a function of the pore volume fraction using data points from Fig. 7. The flexural strength decreased with increasing porosity. According to a model proposed by Rice [39] based on the minimum solid area approach, the strength of a porous material is related to its porosity through the expression

$$\sigma = \sigma_0 \exp(-bP) \quad (1)$$

where σ_0 and σ are the strengths of nonporous and porous materials, respectively, P is the porosity of the porous material, and b is a constant that is dependent on the pore characteristics. The values of b were reported to be 6 for cubic stacking and 9 for rhombic stacking [40]. Linear-regression fits for the plots of flexural strength versus pore volume fraction in Fig. 8 yields $b=10.52$ for the porous SiC ceramics. Previous work on porous SiO_2-bonded SiC ceramics by She et al. [41] and Chun and Kim [30] reported b values of 6.54–7.95. However, the b value in Fig. 5(a) ($b=10.52$) was greater than those reported in the literature for porous SiC ceramics. The most likely explanation for this deviation from the model is that sodium borate is in a different state in each specimen (no melting at 650 and 700 °C, compared to melting in the samples sintered at higher temperatures), which led to a different solid area for each specimen, irrespective of the material porosity.

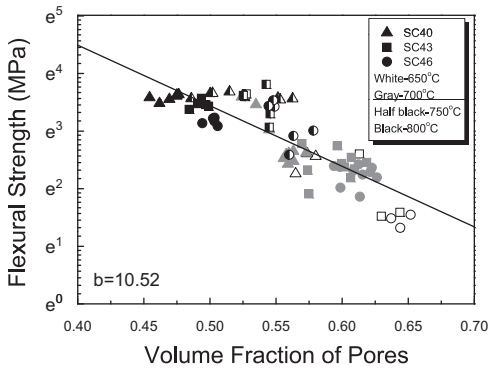

Fig. 8. Flexural strength data of the porous SiC ceramics as a function of pore volume fraction.

There have been many reports on low temperature processing of porous SiC ceramics using many different bonding phases. Table 2 summarizes bonding materials, processing conditions, porosity and flexural (or compressive) strength of porous SiC ceramics processed at temperatures below or equal to 1000 °C. As shown, low temperature processing, at 800–1000 °C, was possible when using preceramic polymers as a bonding material. The obtained strengths of the SiOC-bonded SiC ceramics were 3–22 MPa at 43–56% porosity [35,36]. Soy et al. [42] reported porous bentonite-bonded SiC ceramics. Compressive strengths of the porous ceramics were 0.1–2.5 MPa at 84–86% porosity. Yamane et al. [43] also reported low temperature processing (900 °C) of porous SiC ceramics with pores shaped with Si templates. Typical flexural strength of the porous ceramics was 14 MPa at 61% porosity [43]. In contrast, typical flexural strengths of the present sodium-borate-bonded SiC ceramics fabricated from coarse (cheap) powders (~10 μm) at 750 °C ranged from 25 to 37 MPa at 52–56% porosity, depending on the template content. Furthermore, the sintering time was very short (0.5 h) and the atmosphere used was air. The only material processed at lower temperature than the present study was alkali-bonded SiC [37], in which an alkali

Table 2
Processing conditions, porosity, and flexural strength of porous SiC ceramics fabricated at temperatures below 1500 °C.

Material	Processing conditions (temperature/time/atmosphere)	Porosity (%)	Flexural strength (*Compressive strength) (MPa)	Reference
Sodium borate-bonded SiC	750 °C/0.5 h/Air	52–56	25–37	This study
Alkali-bonded SiC	80 °C/24 h/Air	78–83	0.9*	[37]
SiOC-bonded SiC	1000 °C/1 h/N_2	43–50	3–22	[35]
SiOC-bonded SiC	800 °C/1 h/N_2	52–56	6–18	[36]
Bentonite-bonded SiC	600–1300 °C/2 h/Air	84–86	0.1–2.5*	[42]
SiC (Sodium fluxed)	900 °C/24 h/Ar	61	14	[43]

aluminosilicate binder (also known as geopolymer) was used and processed at 80 °C for 24 h in air. However, typical flexural strength of the material was very low (0.9 MPa of compressive strength). The porous SiC ceramics using sodium borate as a bonding phase developed here have several advantages. First, the processing temperature and holding time during sintering are very low (600–800 °C) and short (0.5 h), respectively. Second, particle size of the starting SiC powder was ~10 μm (cheap). Third, the sintering atmosphere was air. Finally, they have superior strength (37 MPa at 52% porosity) over other refractory-grade SiC ceramics processed at temperatures above 1100 °C. The above advantages make this material cost-effective compared to other porous SiC ceramics for preform fabrication of polymer matrix composites. The SiC-polymer matrix composite can be used as a ceramic brush for grinding the surface of printed circuit boards and some other grinding applications.

4. Conclusions

Porous SiC ceramics with porosities ranging from 47% to 64% were successfully fabricated from SiC–sodium borate–starch mixtures at temperatures as low as 600–800 °C using a simple pressing and heat-treatment process. The microstructures consisted of large SiC grains, sodium borate bonding phase, and pores templated from starch. Increased starch content improved porosity and decreased the flexural strength. The flexural strength generally increased with increased sintering temperature and was maximum at 750 °C. The decrease in the flexural strength of the samples sintered at 800 °C, compared to those sintered at 750 °C, was due to the formation of an oxidation product (SiO_2, cristobalite) in the samples. A porous SiC ceramic with a flexural strength of 37 MPa and a porosity of 52% was obtained by heat treatment in air at 750 °C with a holding time of 0.5 h.

Acknowledgment

This study was supported financially by the Fundamental Research Program of the Korean Institute of Materials Science (KIMS).

References

[1] A.R. Studart, U.T. Gonzenbach, E. Tervoort, L.J. Gauckler, Processing Routes to Macroporous Ceramics: A Review, Journal of the American Ceramic Society 89 (2006) 1771–1789.
[2] T. Ohji, M. Fukushima, Macro-porous ceramics: processing and properties, International Materials Reviews 57 (2012) 115–131.
[3] J. Adler, Ceram diesel particulate filter, International Journal of Applied Ceramic Technology 2 (2005) 429–439.
[4] R. Mouazer, S. Mullens, I. Thijs, J. Luyten, A. Buekenhoudt, Silicon carbide foams by polyurethane replica technique, Advanced Engineering Materials 7 (2005) 1124–1128.
[5] T.E. Wilkes, M.L. Young, R.E. Sepulveda, D.C. Dunand, K.T. Faber, Composites by aluminum infiltration of porous silicon carbide derived from wood precursors, Scripta Materialia 55 (2006) 1083–1086.
[6] R.A. Wach, M. Sugimoto, M. Yoshikawa, Formation of silicon carbide membrane by radiation curing of polycarbosilane an polyvinylsilane and its gas separation up to 250 °C, Journal of the American Ceramic Society 90 (2007) 275–278.
[7] X. Yao, S. Tan, X. Zhang, Z. Huang, D. Jiang, Low-temperature sintering of SiC reticulated porous ceramics with $MgO–Al_2O_3–SiO_2$ additives as sintering aids, Journal of Materials Science 42 (2007) 4960–4966.
[8] R. Dhiman, V. Petrunin, K. Rana, P. Morgen, Conversion of wood structures into porous SiC with shape memory synthesis, Ceramics International 37 (2011) 3281–3289.
[9] S. Ding, Y.P. Zeng, D. Jiang, Gas permeability behavior of mullite-bonded porous silicon carbide ceramics, Journal of Materials Science 42 (2007) 7171–7175.
[10] M. Fukushima, Y. Zhou, Y. Yoshizawa, K. Hirao, Water vapor corrosion behavior of porous silicon carbide membrane support, Journal of the European Ceramic Society 28 (2008) 1043–1048.
[11] M. Fukushima, Y. Zhou, Y.I. Yoshizawa, Fabrication and microstructural characterization of porous SiC membrane supports with $Al_2O_3–Y_2O_3$ additives, Journal of Membrane Science 339 (2009) 78–84.
[12] B.V.M. Kumar, Y.W. Kim, Processing of polysiloxane-derived porous ceramics: a review, Science and Technology of Advanced Materials 11 (2010) 044303.
[13] M. Fukushima, M. Nakata, Y. Zhou, T. Ohji, Y. Yoshizawa, Fabrication and properties of ultra highly porous silicon carbide by the gelation-freezing method, Journal of the European Ceramic Society 30 (2010) 2889–2896.
[14] J.F. Qiu, J.T. Li, K.L. Smirnov, Combustion synthesis of high porosity SiC foam with nanosized grains, Ceramics International 36 (2010) 1901–1904.
[15] A. Dey, N. Kayal, O. Chakrabarti, Preparation of porous SiC ceramics by an infiltration technique, Ceramics International 37 (2011) 223–230.
[16] V. Medri, A. Ruffini, The influence of process parameters on in situ inorganic foaming of alkali-bonded SiC based foams, Ceramics International 38 (2012) 3351–3359.
[17] X. Guo, H. Yang, Y. Huang, L. Zhang, Microstructure and properties of pore-created SiC ceramics with calcium chloride as pore former, Ceramics International 39 (2013) 1299–1305.
[18] G. Amaral-Labat, C. Zollfrank, A. Ortona, S. Pusterla, A. Pizzi, V. Fierro, A. Celzard, Structure and oxidation resistance of microcellular Si–SiC foams derived from natural resins, Ceramics International 39 (2013) 1841–1851.
[19] L. Esposito, D. Sciti, A. Piancastelli, A. Bellosi, Microstructure and properties of porous β-SiC template from soft woods, Journal of the European Ceramic Society 24 (2004) 533–540.
[20] D.A. Streitwieser, N. Popovska, H. Gerhard, Optimization of the ceramization process for the production of three-dimensional biomorphic porous SiC ceramics by chemical vapor infiltration (CVI), Journal of the European Ceramic Society 26 (2006) 2381–2387.
[21] N. Popovska, E. Alkhateeb, A.P. Froba, A. Leipertz, Thermal conductivity of porous SiC composite ceramics derived from paper precursor, Ceramics International 36 (2010) 2203–2207.
[22] L. Biasetto, P. Colombo, M.D.M. Innocentini, S. Mullens, Gas permeability of microcellular ceramic foams, Industrial and Engineering Chemistry Research 46 (2007) 3366–3372.
[23] J.H. Eom, Y.W. Kim, I.H. Song, Effects of the initial α-SiC content on the microstructure, mechanical properties, permeability of macroporous silicon carbide ceramics, Journal of the European Ceramic Society 32 (2012) 1283–1290.
[24] Y.W. Kim, S.H. Kim, C. Wang, C.B. Park, Fabrication of microcellular ceramics using gaseous carbon dioxide, Journal of the American Ceramic Society 86 (2003) 2231–2233.

[25] M. Fukushima, P. Colombo, Silicon carbide-based foams from direct blowing of polycarbosilane, Journal of the European Ceramic Society 32 (2012) 503–510.
[26] S.H. Chae, Y.-W. Kim, I.H. Song, H.D. Kim, M. Narisawa, Porosity control of porous SiC ceramics, Journal of the European Ceramic Society 29 (2009) 2867–2872.
[27] P. Colombo, G. Mera, R. Riedel, G.D. Soraru, Polymer-derived ceramics: 40 years of research and innovation in advanced ceramics, Journal of the American Ceramic Society 93 (2010) 1805–1837.
[28] Y.J. Jin, Y.W. Kim, Low temperature processing of highly porous silicon carbide ceramics with improved flexural strength, Journal of Materials Science 45 (2010) 282–285.
[29] J.H. She, J.F. Yang, N. Kondo, T. Ohji, S. Kanzaki, Z.Y. Deng, High-strength porous silicon carbide ceramics by an oxidation-bonding technique, Journal of the American Ceramic Society 85 (2002) 2852–2854.
[30] Y.S. Chun, Y.-W. Kim, Processing and mechanical properties of porous silica-bonded silicon carbide ceramics, Metals and Materials International 11 (2005) 351–355.
[31] Y. Zhang, Microstructures and mechanical properties of silicon nitride bonded silicon carbide ceramic foams, Materials Research Bulletin 39 (2004) 755–761.
[32] S. Ding, S. Zhu, Y. Zeng, D. Jiang, Effect of Y_2O_3-addition on the properties of reaction-bonded porous SiC ceramics, Ceramics International 32 (2006) 461–466.
[33] S. Liu, Y.P. Zeng, D. Jiang, Effects of CeO_2 addition on the properties of cordierite-bonded porous SiC ceramics, Journal of the European Ceramic Society 29 (2009) 1795–1802.
[34] S. Zhu, S. Ding, H. Xi, R. Wang, Low-temperature fabrication of porous SiC ceramics by preceramic polymer reaction bonding, Materials Letters 59 (2005) 595–597.
[35] Y. Ma, Q.S. Ma, J. Suo, Z.H. Chen, Low-temperature fabrication and characterization of porous SiC ceramics using silicone resin as binder, Ceramics International 34 (2008) 253–255.
[36] J.H. Eom, Y.W. Kim, Low-temperature processing of silicon oxycarbide-bonded silicon carbide, Journal of the American Ceramic Society 93 (2010) 2463–2466.
[37] V. Medri, A. Ruffini, Alkali-bonded SiC based foams, Ceramics International 32 (2012) 1907–1913.
[38] Y.W. Kim, Y.J. Jin, Y.S. Chun, I.H. Song, H.D. Kim, A simple pressing route to closed-cell microcellular ceramics, Scripta Materialia 53 (2005) 921–925.
[39] R.W. Rice, Comparison of stress concentration versus minimum solid area based mechanical property-porosity relations, Journal of Materials Science 28 (1993) 2187–2190.
[40] F.P. Knudsen, Dependence of mechanical strength of brittle polycrystalline specimens on porosity and grain size, Journal of the American Ceramic Society 42 (1959) 376–387.
[41] J.H. She, Z.Y. Deng, J. Daniel-Doni, T. Ohji, Oxidation bonding of porous silicon carbide ceramics, Journal of Materials Science 37 (2002) 3615–3622.
[42] U. Soy, A. Demir, F. Caliskan, Effect of bentonite addition on fabrication of reticulated porous SiC ceramics for liquid metal infiltration, Ceramics International 37 (2011) 15–19.
[43] H. Yamane, T. Shirai, H. Morito, T. Yamada, Y. Hasegawa, T. Ikeda, Fabrication of porous SiC ceramics having pores shaped with Si grain templates, Journal of the European Ceramic Society 31 (2011) 409–413.